

# Vapor-liquid coexistence of patchy models: Relevance to protein phase behavior

Hongjun Liu and Sanat K. Kumar<sup>a)</sup>

*Department of Chemical Engineering, Columbia University, New York, New York 10027*

Francesco Sciortino

*Department of Physics, University of Roma La Sapienza, 00185 Roma, Italy  
and INFM-CNR-SOFT, University of Roma La Sapienza, 00185 Roma, Italy*

(Received 29 May 2007; accepted 9 July 2007; published online 22 August 2007)

The vapor-liquid coexistence boundaries of fluids composed of particles interacting with highly directional patchy interactions, in addition to an isotropic square well potential, are evaluated using grand canonical Monte Carlo simulations combined with the histogram reweighting and finite size scaling methods. We are motivated to study this more complicated model for two reasons. First, it is established that the reduced widths of the metastable vapor-liquid coexistence curve predicted by a model with only isotropic interparticle interactions are much too narrow when compared to the experimental phase behavior of protein solutions. Second, interprotein interactions are well known to be “patchy.” Our results show that at a constant total areal density of patches, the critical temperature and the critical density increase monotonically with an increasing number of uniformly spaced patches. The vapor-liquid coexistence curves plotted in reduced coordinates (i.e., the temperature and the density scaled by their respective critical values) are found to be effectively independent of the number of patches, but are much broader than those found for the isotropic models. Our findings for the reduced width of the coexistence curve are almost in quantitative agreement with the available experimental data for protein solutions, stressing the importance of patchiness in this context. © 2007 American Institute of Physics. [DOI: 10.1063/1.2768056]

## I. INTRODUCTION

The simplest model for describing the attraction between colloid spheres induced by the presence of nonadsorbing polymer<sup>1</sup> is an isotropic square well potential. This model has also been proposed as being useful in describing the phase behavior of model proteins in aqueous solutions.<sup>2–4</sup> Although the phase diagram of globular proteins is qualitatively well reproduced by such isotropic models, a more detailed comparison shows that the predicted reduced widths of the vapor-liquid phase boundary are much too narrow relative to experiment. (Note that the vapor-liquid coexistence curve in these situations is metastable with respect to gas-solid coexistence.) This has led workers to speculate that such models should be improved since they miss, beyond the possible long-range screened electrostatic repulsion,<sup>5</sup> the important physical point that intermolecular interactions between two proteins are highly orientationally specific (or patchy). More recent work has incorporated this aspect and modeled protein molecules as hard spheres with sticky sites on the surface. There has been considerable analytical theory on this simplified model for proteins.<sup>6–10</sup> Similarly, a range of simulation studies<sup>11–16</sup> have studied various models for patchy fluids. The results, in general, suggest that patchy models might adequately describe protein phase behavior. However, a detailed comparison to experiment is missing. Patchy models have also been used to study the sizes and

shapes of crystal nuclei for the formation of solid phases. It has also been found that nucleation rates are exquisitely sensitive to the degree of anisotropy.<sup>17,18</sup>

While the studies discussed above appear to suggest that patchiness has a strong effect on the predicted phase behavior, it is unclear if the inclusion of this effect allows for the proper description of protein phase behavior. Here we focus precisely on such a model and we delineate the locus of the metastable vapor-liquid phase boundary as the number of patches (and their relative positions) on the sphere surface is systematically varied. We present the results of Monte Carlo simulations, using the histogram reweighting method, which show the importance of the number of patches in determining the shape of the vapor-liquid coexistence curve. Their relative placements also appear to play a role in this context. While the number of patches does affect the location of the phase boundary, we find that all of the data for patchy fluids overlap when plotted in reduced coordinates (i.e., normalized by values at the critical point). More importantly, the widths of these reduced plots superpose nicely on the known phase behavior of proteins implicating protein patchiness as being a critical player in determining their phase behavior.

## II. MODEL

We simulate spheres which interact through a combination of an isotropic attraction and sticky patches. Both interactions are described by square well (SW) potentials. The isotropic part is

<sup>a)</sup>Electronic mail: sk2794@columbia.edu

$$u_i(r) = \begin{cases} \infty, & r < \sigma \\ -\varepsilon, & \sigma \leq r < \lambda_i \sigma \\ 0, & r \geq \lambda_i \sigma, \end{cases} \quad (1)$$

where  $\varepsilon$  is the well depth for the isotropic interaction,  $\sigma$  is the particle diameter,  $\lambda_i$  controls the attraction range, and  $r$  is the distance between the centers of mass of the particles. For the patchy part, the potential has both a radial and an angular dependence. Following Kern and Frenkel,<sup>13</sup> we define the interpatch interaction as a product of a square well potential and an angular modulation

$$u_p(r, \Omega_i, \Omega_j) = u^{\text{SW}}(r) \times f(\Omega_i, \Omega_j). \quad (2)$$

The square well part is defined analogous to Eq. (1) but with a different well width,  $\lambda_p$ , and well depth,  $\varepsilon_p$ . The angular part is defined as follows:

$$f(\Omega_i, \Omega_j) = \begin{cases} 1, & \theta_i < \delta \text{ and } \theta_j < \delta \\ 0 & \text{otherwise.} \end{cases} \quad (3)$$

Here  $\theta_i$  is the angle between the line joining the centers of particles and the line connecting the center of particle  $i$  to the center of a patch on its surface.  $\delta$  is the maximum bond-forming angle, which essentially determines the size of patches. To facilitate the comparison between different patch geometries, the areal coverage of the patches,  $\chi$ , is constant for models with different patches,

$$\chi = M \sin^2(\delta/2), \quad (4)$$

where  $M$  is the number of patches. We have varied the number of patches ranging from  $M=4$  to 7 with the following model parameters:  $\lambda_i=1.15$ ,  $\lambda_p=1.05$ ,  $\varepsilon_p=5\varepsilon$ , and  $\chi=0.1$ . The patchy interaction is thus chosen to be shorter ranged than the isotropic one but significantly stronger. Note that this value of  $\chi$  corresponds to  $\delta=0.32$  rad for  $M=4$  and  $\delta=0.24$  rad for  $M=7$ . Such small values ensure that, due to geometric constraints,  $M$  is the maximum number of bonds per particle, i.e., at most one patch pair can interact through a given patch. We have used three different distributions of patches to probe the sensitivity of our findings. The first two are shown in Fig. 1. In the first choice, we have directly employed the packing of a small number of spheres as a means of spacing the patches. The second choice is more arbitrary: it is the same as case 1 for  $M=4$ . However, for  $M=5$  we used a square pyramid, while for  $M=7$  it is a polyhedron with a square bottom and an equilateral triangle top. In a third case, which we shall discuss below, we utilize the patch distribution from case 1, but randomly perturb the positions of the patches. We shall perform most of our studies on set 1, but use the other two sets to understand the sensitivity of the determined critical points to the placement of patches. Simulation results are reported in reduced units as  $T^* = kT/\varepsilon$ ,  $\rho^* = N\sigma^3/V$ , and  $L^* = L/\sigma$ . In what follows, we omit the asterisk for simplicity.

### III. SIMULATION TECHNIQUES

Grand canonical ensemble Monte Carlo (GCMC) simulations and the histogram reweighting method are used to

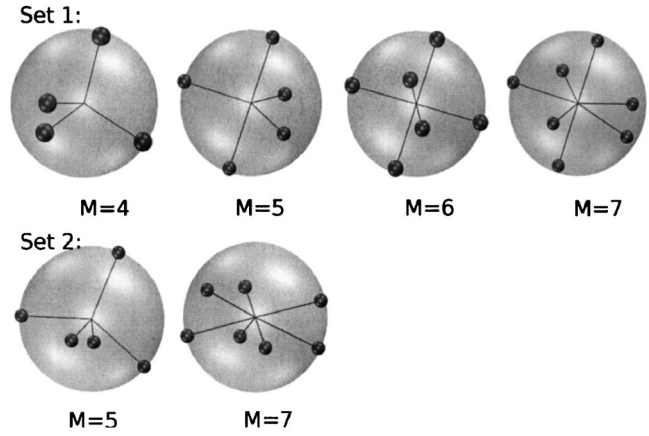


FIG. 1. Schematic representation of the placement of the patchy sites (small spheres) on the surface of the particle (big spheres). The patch geometries for set 1 are chosen as tetrahedron ( $M=4$ ), triangular dipyramid ( $M=5$ ), octahedron ( $M=6$ ), and pentagonal dipyramid ( $M=7$ ) (Ref. 32). The patch geometries for set 2 are taken as the square pyramid ( $M=5$ ) and the polyhedron with square bottom and the equilateral triangle top ( $M=7$ ).

locate the critical point and the phase diagram. In this ensemble the probability of observing a system with a given number of particles  $N$  with energy  $E$  is

$$f(N, E) = \frac{\Omega(N, V, E) \exp(\beta\mu N - \beta E)}{\sum_N \sum_E \Omega(N, V, E) \exp(\beta\mu N - \beta E)}, \quad (5)$$

where  $\Omega(N, V, E)$  is the density of states. In order to cover the broadest range of phase space, multiple simulations are required at various chemical potentials and temperatures. In all cases we assure that the histograms possess sufficient overlap. We derive the optimum density of states by using the method proposed by Ferrenberg and Swendsen,<sup>19,20</sup> from which the phase diagrams can be readily estimated.

To estimate the critical point we employed the finite size scaling method.<sup>15,21–23</sup> According to the mixed-field theory, the relevant ordering operator is a linear combination of the number of particles  $N$  and energy  $E$ :  $X = N - sE$ , where  $s$  is a field mixing parameter controlling the coupling strength between energy and density fluctuations. At the critical point, the fluctuations of this ordering operator are well described by the universal Ising distribution.<sup>24</sup> Fits of our simulation results to this well defined functional form permit for a direct evaluation of the critical parameters for the various  $M$  models. The critical parameters are found to be  $L$  dependent because of corrections to scaling.<sup>22</sup> The deviation of the apparent critical temperature from the true critical temperature is given by  $T_c(L) - T_c(\infty) \propto L^{-(\theta+1)/\nu}$ , with  $\theta=0.54$  (Ref. 25) and  $\nu=0.629$ .<sup>26</sup> A linear least-squares extrapolation of  $T_c$  at a variety of  $L$  values can yield the critical temperature of the infinite system. Similarly, the critical density follows the scaling law:  $\rho_c(L) - \rho_c(\infty) \propto L^{-(d-1)/\nu}$ , where  $d$  is the dimensionality of the system. From here the critical density of a system in the thermodynamic limit can be derived. The simulations were performed for several system sizes  $L=5, 6, 7$ , and  $8\sigma$ . The simulation box is a cube with periodic boundary conditions in all three directions. Each of the simulations is at least  $10^6$  MC steps in length. Each MC step includes 400

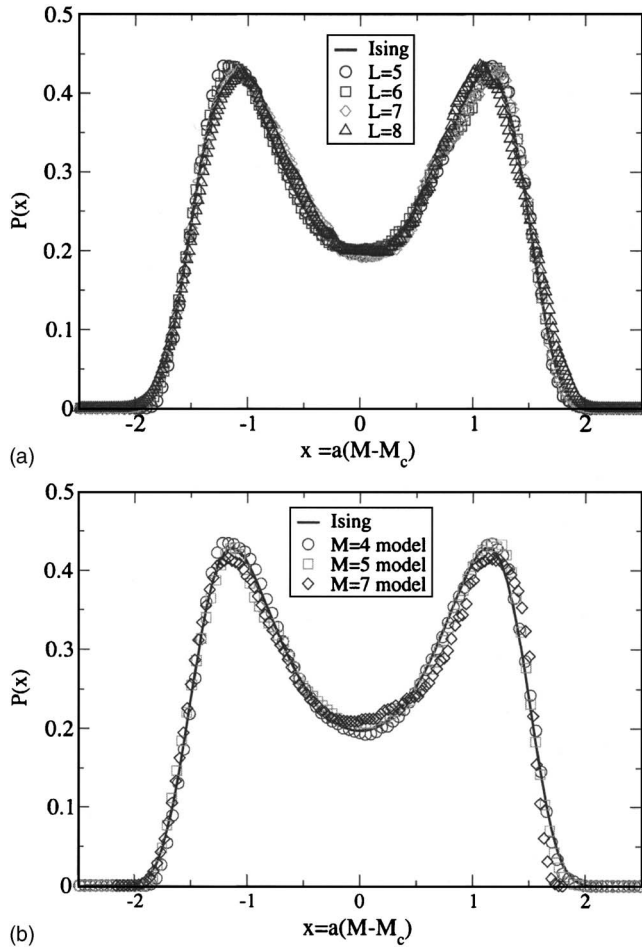


FIG. 2. (a) Distributions of the ordering operator for all studied system sizes at the apparent critical points for the  $M=4$  model. The nonuniversal constant  $a$  and the critical value of the ordering operator  $M_c$  were chosen such that the distributions have zero mean and unit variance. The universal Ising ordering operator distribution  $p_M^*(x)$  is shown by the solid line. (b) Distributions of the ordering operator for the  $M=4$ ,  $M=5$ , and  $M=7$  models at the apparent critical point at the system size  $L=5$ , compared with the universal ordering operator distribution  $p_M^*(x)$  (solid line) of the Ising universality class.

random attempts of rotation/translation and 4 attempts of insertion and deletion. To improve statistics, six independent MC realizations were averaged. In this manner the phase behavior in the thermodynamic limit is recovered.

We have never observed crystallization for  $M=4$ , 5, and 7 fluids for the conditions covered by this study. However, the  $M=6$  fluid with a uniform distribution of patches readily crystallized into a simple cubic form: thus we do not focus on this case except at the end of the paper.

#### IV. RESULTS AND DISCUSSIONS

We first focus on the  $M=4$  model. We show the distribution of the ordering operator ( $X$ ) at the apparent critical points for all system sizes studied. Consistent with expectation, this system's phase behavior belongs to the Ising universality class (see Fig. 2). This matching process allows us to accurately determine the apparent critical point  $T_c(L)$  and  $\mu_c(L)$  and the field-mixing parameter  $s$ . The relevant parameters were summarized in Table I. A size-independent value of  $s=0.028$  allows simultaneous fit of all distributions of the

TABLE I. Values of the relevant parameters at the apparent critical point for the patchy models.

$L$	$T_c(L)$	$\mu_c(L)$	$\rho_c(L)$	$s$
$M=4$				
5	0.811	-2.449	0.3833	0.028
6	0.8115	-2.4457	0.3838	0.028
7	0.812	-2.4449	0.3824	0.028
8	0.8133	-2.4316	0.3830	0.028
$M=5$				
5	0.8445	-2.3845	0.4122	0.015
$M=7$				
5	0.915	-2.126	0.5235	0.0

ordering operator. The fact that  $s$  is small indicates that the extent of field mixing is small, and the distribution of density is nearly symmetric. From estimates of the finite apparent critical points, we can estimate the critical point for the infinite volume system. We find  $T_c(\infty)=0.8137$ ,  $\mu_c(\infty)=-2.433$ , and  $\rho_c(\infty)=0.3822$  for the  $M=4$  model.

Next, we move to the  $M=5$  and  $M=7$  models following the set 1 distribution of patches. For the time being, we only deal with the system size  $L=5$ . We present the distribution of the ordering operator at the apparent critical point in Fig. 2. Although the mixing-field parameter  $s$  is always small, it increases with decreasing  $M$ , in agreement with previous findings.<sup>15</sup> This implies an increasing role of the mixing field and a more asymmetric critical density distribution with a smaller number of patches.

Then, we discuss the resulting vapor-liquid coexistence (VLE) curves. Figure 3 shows the data for the  $M=4$ ,  $M=5$ , and  $M=7$  models and compare it to the isotropic model<sup>27</sup> and a primitive model for water (PMW).<sup>16</sup> Several trends are transparent. Looking at the patchy fluids, it is apparent that both the  $T_c$  and the  $\rho_c$  increase with increasing  $M$  (Fig. 3).

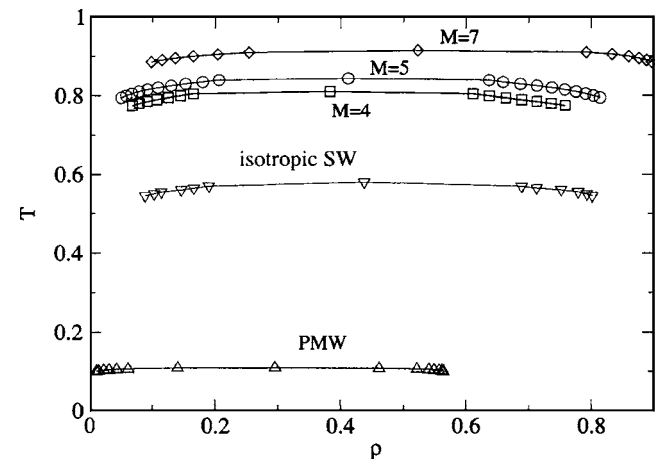


FIG. 3. Vapor-liquid coexistence curves for the studied patchy models  $M=4$  (squares),  $M=5$  (circles), and  $M=7$  (diamonds). Data for the isotropic SW model with  $\lambda=1.15$  (inverted triangles) are from Ref. 27; PMW data (triangles) from Ref. 16. Note that while we used the well depth of the isotropic potential to define the reduced temperature of the isotropic SW and the patchy models studied in this work, we used the patchy interaction well depth in the case of the PMW model since it does not include an isotropic potential.

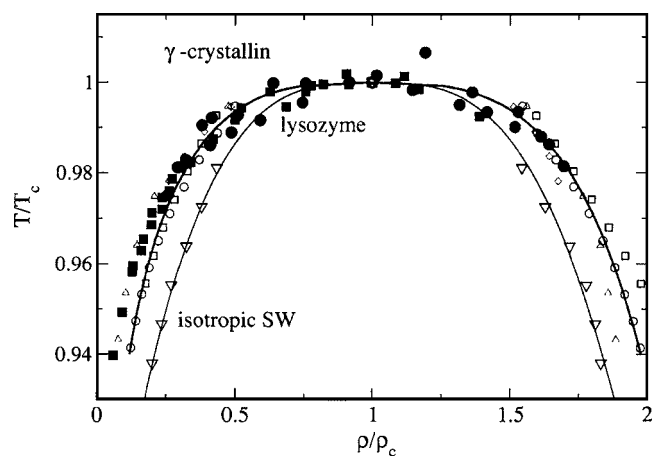


FIG. 4. Vapor-liquid coexistence curves in terms of the reduced temperatures  $T/T_c$  and the reduced density  $\rho/\rho_c$  for the studied patchy models:  $M=4$  (open squares),  $M=5$  (open circles), and  $M=7$  (open diamonds). The isotropic only (Ref. 27) (inverted open triangles) and PMW (Ref. 16) (open triangles) data are shown for comparison. The experimental data for  $\gamma$ -crystallin (full circles) and lysozyme (full squares) are taken from Refs. 28 and 29, respectively. The lines are the fit to the standard critical scaling law used to describe coexistence curves.

This is consistent with the recent findings of Bianchi *et al.*,<sup>15</sup> confirming the strong correlation between the critical density and the effective *valence* of the particles. In comparison with the purely isotropic model the critical density of the  $M=4$  model is lower, while its  $T_c$  is higher. Since the patch interactions provide an additional source of attraction, we expect that the critical temperature, in the presence of patches, will always be higher than the corresponding isotropic case. In the PMW model,<sup>16</sup> the isotropic reference state is the hard core and the critical  $T$  is completely controlled by bonding. In the case of the  $M=4$  fluid we find that the critical density is intermediate between the PMW and the isotropic case, suggesting that both interactions play a role in the location of the critical point.

To examine the effect of  $M$  on the width of the VLE curves, we present the phase diagram in terms of the reduced units in Fig. 4. We also include the simulation data of PMW and the SW model with  $\lambda=1.15$ , and the experimental data for  $\gamma$ -crystallin and lysozyme. The data for all patchy models and the PMW collapse onto a single master curve. These curves are much broader than that of the isotropic only model and show an excellent agreement with the experimental results for  $\gamma$ -crystallin<sup>28</sup> and lysozyme.<sup>29</sup> Thus, we tentatively conclude that patchy models represent a more realistic description of protein-protein interactions even in the context of dilute solution behavior.

Next, we investigate the effect of patch placements on the critical point. The first question we would like to address is if the critical point tolerates small perturbations of patch positions. We chose the set 1 patch design as the starting point, and made small random movement of patches on the surface of particle. The magnitude of the random movement is proportional to the patch size and is set to  $\delta/5$ . The final location of the patches is identical for all particles. The results demonstrate that such small perturbation cause no changes to the critical point within simulation uncertainty.

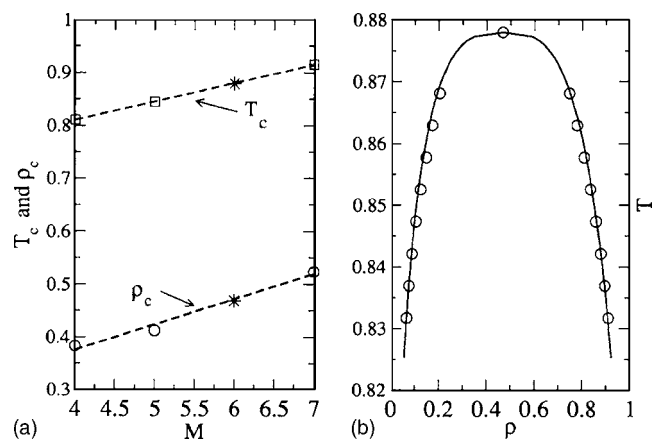


FIG. 5. (a) The dependence of the critical points for patchy models with a variable number of patches. Interpolation (asterisks) yields an estimate for the  $M=6$  model:  $T_c=0.879$  and  $\rho_c=0.4685$ . (b) The estimated vapor-liquid coexistence curve for the  $M=6$  model assuming that all patchy models fall on the master VLE curve in terms of the reduced temperature and density.

We also studied the models in set 2, which have a patch distribution which is quite different from those in set 1. We found that the estimated critical temperatures are different from the counterparts in set 1. The  $M=5$  model in set 2 shows an increase in  $T_c$  by 0.01 and an increase in  $\rho_c$  of 0.02, while  $T_c$  of the  $M=7$  model in set 2 decreases by 0.07 and  $\rho_c$  decreases by  $\approx 0.1$ . Since the  $T_c$  and  $\rho_c$  values appear to be shifted in either direction depending on the specific patch placements, we conclude that patch placement is also playing a role in determining the critical point.

In addition to the understanding that is obtained for the role of patchiness on phase behavior, the results presented here can be used to predict the critical behavior of the  $M=6$  model, which has been excluded by our study. Indeed, we have not focused on  $M=6$ , since this is the only one that crystallizes easily. In all our calculations we found that the  $M=6$  system crystallizes so readily that we have to perform histogram reweighting calculations at high temperatures to suppress crystallization. Extrapolations of histograms from this high temperature do not yield meaningful estimates of the phase diagram. To circumvent this problem and to estimate the phase behavior of this interesting patch model we have estimated its critical temperatures and densities by interpolation of Fig. 5(a). We find  $T_c=0.879$  and  $\rho_c=0.4685$ . Then, by assuming that the phase diagram of the  $M=6$  model falls onto the same master curve shown in Fig. 4 we can estimate the vapor-liquid coexistence curve for this fluid [Fig. 5(b)].

## V. CONCLUSION

We have used Monte Carlo simulations to investigate the vapor-liquid coexistence curves for several patchy models, prototype models for describing interaction between proteins. In the models studied, the isotropic square well attractive potential is complemented by  $M$  independent patch interactions, modeled as in Ref. 13. All studied models are characterized by the same (small) overall patch coverage. The critical density and temperature are found to monotonically decrease as the number of patches decreases, favoring

the establishment of a homogeneous liquid state at intermediate densities,<sup>31</sup> a phenomenon which could favor the formation of disordered arrested states (protein gels). We have observed that these results are less sensitive to the placement of patches than to the number of patches themselves, confirming the important role of the effective *valence* in rationalizing the resulting phase diagram.

We have shown that the phase diagrams of all patchy models studied fall, in reduced units, onto the same master curve, which also appears to coincide with the experimental measures of the metastable vapor-liquid lines for two model proteins. This result stresses the importance of patchy interactions in describing the behavior of proteins, a conclusion that is consistent with the known patchy nature of protein surfaces (and hence interactions). In this respect, the shape of the phase diagram in reduced units can provide an indication of the importance of patchy interactions. The specific values of the critical density can even provide information on the actual number of patches.

Finally, we note that results presented in this article refer to a specific value of the coverage and to a specific ratio of the isotropic to patchy interaction strength. Future studies will address the role of these quantities on the phase diagram of patchy particles.

## ACKNOWLEDGMENTS

The authors thank the National Science Foundation (ITR grant, DMR-0313101) and the Department of Energy for funding this research.

<sup>1</sup>S. Asakura and F. Oosawa, J. Chem. Phys. **22**, 1255 (1954); URL: <http://link.aip.org/link/?JCP/22/1255/2>

<sup>2</sup>A. Lomakin, N. Asherie, and G. B. Benedek, J. Chem. Phys. **104**, 1646 (1996); URL: <http://link.aip.org/link/?JCP/104/1646/1>

<sup>3</sup>N. Asherie, A. Lomakin, and G. B. Benedek, Phys. Rev. Lett. **77**, 4832 (1996).

<sup>4</sup>F. W. Tavares and S. I. Sandler, AIChE J. **43**, 218 (1997).

<sup>5</sup>F. Cardinaux, A. Stradner, P. Schurtenberger, F. Sciortino, and E. Zaccarelli, Europhys. Lett. **77**, 48004 (2007); URL: <http://stacks.iop.org/0295-5075/77/i=4/a=48004>

<sup>6</sup>R. P. Sear, J. Chem. Phys. **111**, 4800 (1999); URL: <http://link.aip.org/link/?JCP/111/4800/1>

<sup>7</sup>R. A. Curtis, H. W. Blanch, and J. M. Prausnitz, J. Phys. Chem. B **105**, 2445 (2001); URL: [http://pubs3.acs.org/acs/journals/doilookup?in\\_doi=10.1021/jp003087j](http://pubs3.acs.org/acs/journals/doilookup?in_doi=10.1021/jp003087j)

<sup>8</sup>A. Lomakin, N. Asherie, and G. B. Benedek, Proc. Natl. Acad. Sci. U.S.A. **96**, 9465 (1999); <http://www.pnas.org/cgi/reprint/96/17/9465.pdf>; URL: <http://www.pnas.org/cgi/content/abstract/96/17/9465>

<sup>9</sup>B. L. Neal, D. Asthagiri, and A. M. Lenhoff, Biophys. J. **75**, 2469 (1998); <http://www.biophysj.org/cgi/reprint/75/5/2469.pdf>; URL: <http://www.biophysj.org/cgi/content/abstract/75/5/2469>

<sup>10</sup>C. Haas, J. Drenth, and W. W. Wilson, J. Phys. Chem. B **103**, 2808 (1999); URL: [http://pubs3.acs.org/acs/journals/doilookup?in\\_doi=10.1021/jp9840351](http://pubs3.acs.org/acs/journals/doilookup?in_doi=10.1021/jp9840351)

<sup>11</sup>C. Vega and P. A. Monson, J. Chem. Phys. **109**, 9938 (1998); URL: <http://link.aip.org/link/?JCP/109/9938/1>

<sup>12</sup>X. Song, Phys. Rev. E **66**, 011909 (2002).

<sup>13</sup>N. Kern and D. Frenkel, J. Chem. Phys. **118**, 9882 (2003); URL: <http://link.aip.org/link/?JCP/118/9882/1>

<sup>14</sup>J. Chang, A. M. Lenhoff, and S. I. Sandler, J. Chem. Phys. **120**, 3003 (2004); URL: <http://link.aip.org/link/?JCP/120/3003/1>

<sup>15</sup>E. Bianchi, J. Largo, P. Tartaglia, E. Zaccarelli, and F. Sciortino, Phys. Rev. Lett. **97**, 168301 (2006); URL: <http://link.aps.org/abstract/PRL/v97/e168301>

<sup>16</sup>F. Romano, P. Tartaglia, and F. Sciortino, J. Phys.: Condens. Matter **19**, 322101 (2007); URL: <http://stacks.iop.org/0953-8984/19/i=32/a=322101>

<sup>17</sup>V. Talanquer, J. Chem. Phys. **122**, 084704 (2005); URL: <http://link.aip.org/link/?JCP/122/084704/1>

<sup>18</sup>N. M. Dixit and C. F. Zukoski, J. Chem. Phys. **117**, 8540 (2002); URL: <http://link.aip.org/link/?JCP/117/8540/1>

<sup>19</sup>A. M. Ferrenberg and R. H. Swendsen, Phys. Rev. Lett. **61**, 2635 (1988).

<sup>20</sup>A. M. Ferrenberg and R. H. Swendsen, Phys. Rev. Lett. **63**, 1195 (1989).

<sup>21</sup>N. B. Wilding and A. D. Bruce, J. Phys.: Condens. Matter **4**, 3087 (1992); URL: <http://stacks.iop.org/0953-8984/4/3087>

<sup>22</sup>N. B. Wilding, J. Phys.: Condens. Matter **9**, 585 (1997); URL: <http://stacks.iop.org/0953-8984/9/585>

<sup>23</sup>M. A. Miller and D. Frenkel, Phys. Rev. Lett. **90**, 135702 (2003).

<sup>24</sup>M. M. Tsy-pin and H. W. J. Blöte, Phys. Rev. E **62**, 73 (2000).

<sup>25</sup>J.-H. Chen, M. E. Fisher, and B. G. Nickel, Phys. Rev. Lett. **48**, 630 (1982).

<sup>26</sup>A. M. Ferrenberg and D. P. Landau, Phys. Rev. B **44**, 5081 (1991).

<sup>27</sup>H. Liu, S. Garde, and S. Kumar, J. Chem. Phys. **123**, 174505 (2005); URL: <http://link.aip.org/link/?JCP/123/174505/1>

<sup>28</sup>M. L. Broide, C. R. Berland, J. Pande, O. O. Ogun, and G. B. Benedek, Proc. Natl. Acad. Sci. U.S.A. **88**, 5660 (1991); <http://www.pnas.org/cgi/reprint/88/13/5660.pdf>; URL: <http://www.pnas.org/cgi/content/abstract/88/13/5660>

<sup>29</sup>D. N. Petsev, X. Wu, O. Galkin, and P. G. Vekilov, J. Phys. Chem. B **107**, 3921 (2003); URL: [http://pubs3.acs.org/acs/journals/doilookup?in\\_doi=10.1021/jp0278317](http://pubs3.acs.org/acs/journals/doilookup?in_doi=10.1021/jp0278317)

<sup>30</sup>D. Costa, P. Ballone, and C. Caccamo, J. Chem. Phys. **116**, 3327 (2002); URL: <http://link.aip.org/link/?JCP/116/3327/1>

<sup>31</sup>E. Zaccarelli, S. Buldyrev, E. La Nave, A. Moreno, I. Saika-Voivod, F. Sciortino, and P. Tartaglia, Phys. Rev. Lett. **94**, 218301 (2005).

<sup>32</sup>V. N. Manoharan, M. T. Elsesser, and D. J. Pine, Science **301**, 483 (2003); <http://www.sciencemag.org/cgi/reprint/301/5632/483.pdf>; URL: <http://www.sciencemag.org/cgi/content/abstract/301/5632/483>